Distinct Dynamic Behaviors of Water Molecules in Hydrated Pores

ARTICLE *in* JOURNAL OF THE AMERICAN CHEMICAL SOCIETY · SEPTEMBER 2006

Impact Factor: 12.11 · DOI: 10.1021/ja063223j · Source: PubMed

Supporting Information for the communication entitled

Distinct Dynamic Behaviors of Water Molecules in Hydrated Pores

by

Martín Febles,[†] Natalia Pérez-Hernández,[‡] Cirilo Pérez,[†] Matías L. Rodríguez,[†] Concepción Foces-Foces,[⊥] María Victoria Roux,[⊥] Ezequiel Q. Morales,[‡] Gerd Buntkowsky,[#] Hans-Heinrich Limbach,[§] and Julio D. Martín.*[,‡]

[†]Instituto de Bioorgánica, Universidad de La Laguna-CSIC, Ctra. Vieja de La Esperanza 2, 38206 La Laguna, Tenerife, Spain, [‡]Instituto de Investigaciones Químicas, CSIC, Avda. Américo Vespucio s/n, 41092 Seville, Spain, [⊥]Instituto de Química-Física Rocasolano, CSIC, Serrano 119, 28006 Madrid, Spain, [#]Institut für Physikalische Chemie, Friedrich-Schiller Universität, Helmholtzweg 4, D-07743 Jena, Germany and [§]Institut für Chemie, Freie Universität Berlin, Takusstr. 3, D-14195 Berlin, Germany

1 Solid state NMR results on tubular structure formed by (±)**1**·2H_2O

1.1 ^{1}H and ^{2}H MAS NMR experiments

A series of ^{1}H MAS experiments (600 MHz, spin rate = 24 kHz) were performed using differently treated samples of (±)**1**·2H_2O

Crystals containing the tubular structures gave rise to the spectrum shown in figure 1a, where the acidic and alcoholic mobile proton sites can be identified. In contrast, no structural water signal is observed due to its motion rate under these conditions. The spectrum of the same sample submitted to high vacuum[1] exhibits a greater distribution of signals because of structural changes in the pore-like assembly caused by the removal of water (figure 1b). In agreement with results obtained by calorimetric experiments, the presence of water is necessary for the tubular structure to be held together.

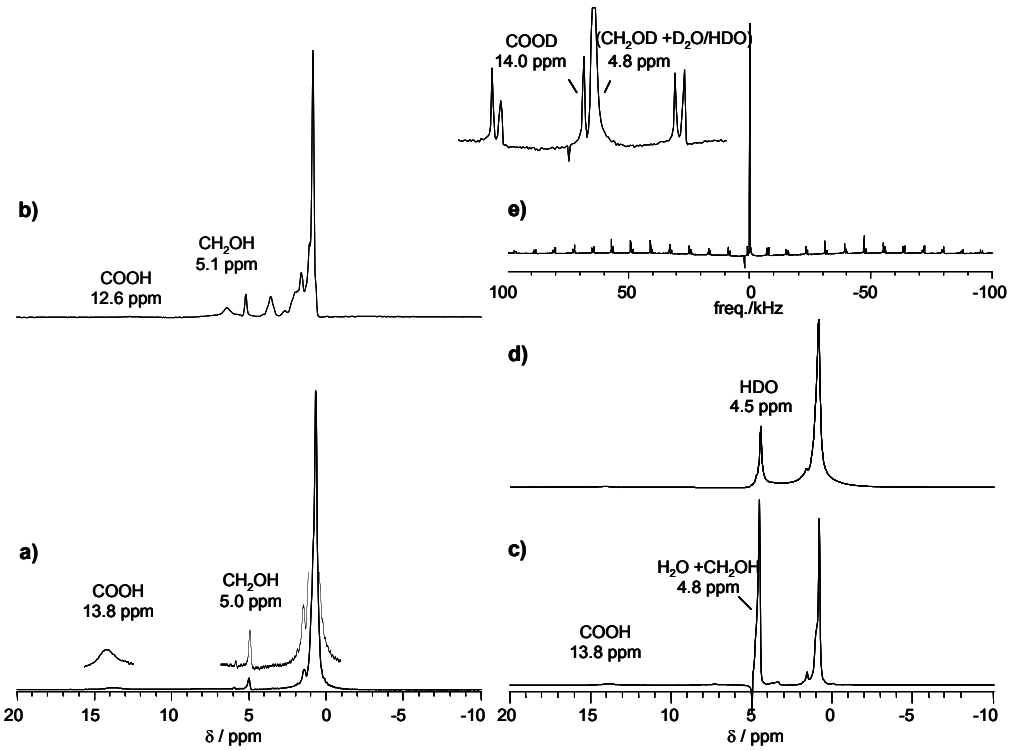

Figure 1: a) ^{1}H MAS NMR spectrum of a tubular compound formed by (±)**1**·2H_2O with expansion of alcoholic and acidic ^{1}H signals. b) ^{1}H MAS NMR spectrum of (±)**1**·2H_2O after being submitted to high vacuum overnight. c) ^{1}H MAS NMR spectrum of (±)**1**·2H_2O after exposure to H_2O vapor. d) ^{1}H MAS NMR spectrum of (±)**1**·2H_2O after exposure to D_2O vapor. e) Complementary ^{2}H spectrum of sample d) with expansion of central band.

Exposure of (±)**1**·2H_2O crystals to H_2O or D_2O vapor does not alter the pore structure, as inferred from the known resulting ^{1}H spectra of the treated samples (figures 1c and 1d). Furthermore, it results in the acquisition of a large number of water

[1] The sample was exposed to 10^{-7} mbar overnight.

molecules exhibiting a high degree of mobility inside the pore and giving rise to sharp and intense signals. The isotropic signal in the complementary ^{2}H spectrum (spin rate = 12 kHz), of the sample exposed to D_2O vapor (figure 1e) indicates bulk-water behavior[2] of these water molecules.

By means of exposing the sample to gaseous D_2O at a lower vapor pressure, the mobile proton sites of the tubular structure can be partially deuterated without the entry of a great number of water molecules (figures 2a and 2b).

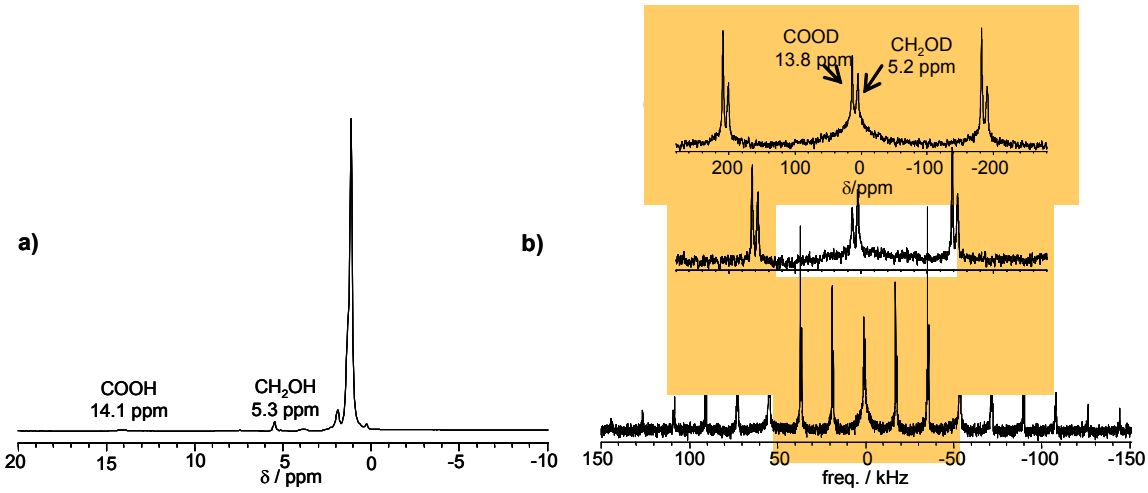

Figure 2: a) ^{1}H MAS NMR spectrum of crystals of (±)**1**·2H_2O exposed to D_2O vapor, showing the expected appearance for the pore-forming sample. b) ^{2}H MAS NMR spectrum of the same sample with expansion of central bands for a clear view of the deuterated alcoholic and acidic mobile sites.

1.2 Solid State Static ^{2}H NMR results

In a row of static ^{2}H NMR[3] experiments (300 MHz), a sample of (±)**1**·2H_2O treated in such a way is used to verify the presence of structural water molecules moving across their sites in the walls of the pore, and thus not observed in any of the above -mentioned spectra. At room temperature, only a small fraction of water molecules in the form of clusters or "mini-droplets" inside the pore can be observed as low intensity, and, in some case, isotropic signals. As expected, the largest water amount is not observable until the temperature is lowered to 223 K. The incorporation of the structural water signal to the spectrum at low temperatures produces a great increase in the alcoholic OD signal intensity, which showed a 1:1 ratio when compared to the acidic COOD signal

[2] The intense and sharp line in the central band of the ^{2}H spectrum does not appear in the spinning sidebands, indicating isotropic behavior of the D_2O molecules.

[3] See combined static ^{2}H NMR and calorimetric experiments for identifying water molecules exhibiting different motion rates: (a) Su, C.-Y.; Goforth, A.M.; Smith, M.D.; Pellechia, P.J.; zur Loye, H.-C. *J. Am. Chem. Soc*. **2004**, *126*, 3576-3586; (b) Cheruzel, L. E.; Pometun, M. S.; Cecil, M.R.; Mashuta, M. S.; Wittebort, R.J.; Buchanan, R.M.; *Angew. Chem. Int. Ed*. **2003**, *42*, 5452-5455.

intensity at room temperature[4] (figures 3a and 3b). This change of the structural water motion is observed for several samples treated in the same way, and takes place lineally in the expected temperature interval according to DSC experiments (see figure 3c).[5]

Besides, the broadening of the signals corresponding to the small water fraction in the form of clusters or mini-droplets[6] shows the temperature influence on the motion of these water molecules.

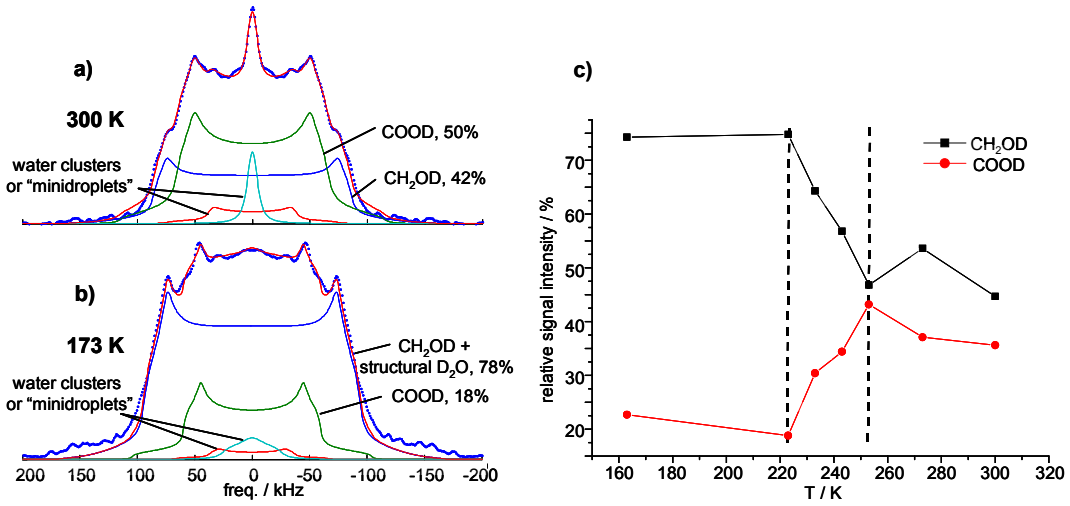

Figure 3: a) and b) Superposition of static ^{2}H NMR spectra and simulations of individual signals at 300 K and 173 K respectively. Assignment of deuterated water, alcoholic and acidic functions as well as relative intensity percentages are depicted. c) Graph with representation of CH_2OD and COOD relative signal intensities versus temperature for a series of static ^{2}H NMR experiments. The linear change of intensities takes place in the enhanced temperature interval.

1.3 Kinetics of the deuteration process followed by Solid State Static ^{2}H NMR

The sample is exposed for 15 minutes, 30 minutes, 1h and 2.5 h to D_2O vapor. Only after 2.5 h is there a visible deuterium signal. The same sample is afterwards exposed for 11 h, thus 13.5 h altogether. During this time, the sample undergoes a weight increase of 3.2%. The spectra and the simulations are shown in figure 4.

---

[4] Signals have been assigned according to the known ^{2}H MAS spinning sideband pattern as well as considering hydrogen bond strengths and distances correlated to quadrupolar coupling constants: (a) Brunner, E.; Sternberg, U., *Progr. NMR. Spect.* **1998**, *32*, 21-57. (b) Chiba, T. *J. Chem. Phys*. **1964**, *41,* 1352-1358. (c) Chiba, T.; Soda, G. *Bull. Chem. Soc. Jpn*. **1971**, *44*, 1703-1705. (d) Berglund, B.; Vaughan, R.W. *J. Chem. Phys*. **1980**, *73*, 2037-2043. (e) Seliger, J.; Žagar, V.; Blinc, R. *Chem. Phys. Lett*. **1984**, *104*, 277-278.

[5] This methodology has been used to study the motion of water in ice and allows estimating correlation times of microseconds for the structural water molecules in our sample: Wittebort, R.J.; Usha, M.G.; Ruben, D.J.; Wemmer, D.E., Pines, A. *J. Am. Chem. Soc*. **1988**, 110, 5668-5671.

[6] For examples of the NMR characterization of water molecules with different motion rates, see: (a) Klug, C.A.; Lee, P.L.; Lee, I.-S. H.; Kreevoy, M.M.; Yaris, R.; Schaefer, J. *J. Phys. Chem. B* **1997**, *101*, 8086-8091. (b) Grünberg, B.; Emmler, T.; Gedat, E.; Shenderovich, I.; Findenegg, G.H.; Limbach, H.-H.; Buntkowsky, G. *Chem. Eur. J.* **2004**, 10, 5689-5696.

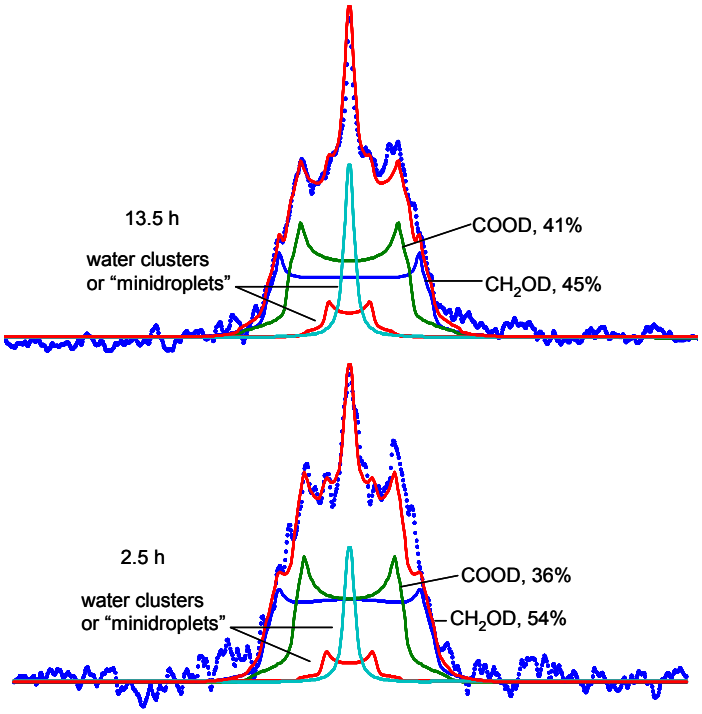

Figure 4: Room temperature static ^{2}H spectrum and simulation of sample exposed for 2.5 h (down) and for 13.5h (up) to D_2O. Signal intensities are depicted. Note how after 13.5 h the OD and COOD positions are already deuterated to the same extent and have the same appearance as the spectra recorded after days of exposure.

1.4 Experimental

1.4.1 MAS NMR experiments

For the experiments with the "standard" (±)**1**·2H_2O sample, around 10 mg of crystals grown from a CCl_4/ n-hexane interface were simply introduced in the rotor. In the case of samples exposed to H_2O or D_2O vapor, and samples submitted to vacuum, the substance was rapidly introduced in the rotor immediately prior to the measurement. Exposure to H_2O or D_2O was achieved by means of introducing the sample in an open eppendorf which in turn was placed in a small desiccator containing approximately 10 ml of H_2O or D_2O. The whole system was kept at 40 ºC over several days. In all cases a Varian 600 MHz Infinity Plus spectrometer was used equipped with Spinsight Software (version 4.3.2), and a 3.2 mm HX-T3 Chemmagnetics probehead. The spin rate was 24 kHz in the ^{1}H experiments (stabilized by the spectrometer), a spin-echo pulse sequence (echo delay = 833 μs = 20 rotor cycles, ns = 512, pulse delay = 6 s) was used, and TSP was the reference for the chemical shift. Even using a spin-echo sequence, a signal corresponding to the empty rotor was observed in the spectra. For this reason, all measurements had to be completed with a parallel experiment of the empty rotor, and its

signal was afterwards subtracted to obtain the spectrum only with the actual sample signals.

For typical ^{2}H experiments, spin rates of 8 to18 kHz, 1 pulse experiments (pd = 6 s, ns = 12000), and deuterated polystyrene for the chemical shift reference were used.

1.4.2 Solid State Static ^{2}H NMR experiments

In this case approximately 150 mg of substance were introduced in an NMR tube which was sealed 1.5 cm above the top of the substance, in order to avoid exchange of the deuterated sample with environmental H_2O. The static ^{2}H experiments were performed using a home built 5 mm ^{2}H-NMR probe. The probe is placed in a dynamic Oxford CF1200 helium flow cryostat. The sample temperature was controlled employing an Oxford ITC 503 temperature controller. Spin-echo experiments with optimized parameters for a deuterated polystyrene sample were performed, using pulse delays between 1 s and 20 s (increasing the delay when lowering temperature), and using 5000 accumulations (for long pulse delays) and 50000 accumulations (for short pulse delays).

2 DSC and TG results for compounds (±)**1**·2H_2O and (±)**2**·2H_2O

2.1 DSC results for compound (±)**1**·2H_2O

Table 1: DSC experiment performed on a (±)**1**·2H_2O sample.

process	rate K/min	modification 1			modification 2		
		temp.interval *T*/ K	T_{peak} K	$\Delta H°$ J/g	temp.interval *T*/ K	T_{peak} K	$\Delta H°$ J/g
1st cooling	5						
1st heating	10	197.1→ 273.0	246.4	5.4	273.0→ 292.2	279.8	0.5
2nd cooling	10						
2nd heating	10	194.7 → 265.3	232.4	5.1	270.0 →288.5	275.1	0.6
3rd cooling	20						
3rd heating	10	194.7 → 260.7	240.4	3.0	260.7 →288.3	272.4	0.7

Two enthalpic modifications are observed in three different heating processes at 10 K/min. Increasing cooling rates have been used before each heating process.

The most important enthalpic variation, depicted as **modification 1**, occurs in all cases in approximately similar temperature intervals to those observed by ^{2}H NMR to correspond with changes in the structural water molecules motion along their wall sites (Table 1). The basic pore structure remains unaltered at these temperatures. This fact, added to the reversibility of the process (shown by the consecutive results with the same sample), identifies indeed **modification 1** with changes in the structural water behavior.

Another enthalpic change, **modification 2**, is observed around 0 ºC with a lower ΔH^o value, related to fusion-freezing processes described for water confined in pores at these temperatures.[7] In our case it corresponds with the presence of water mini-droplets inside the pore.

2.2 DSC results for the compound of (±)**2**·2H_2O

Table 2: Experiment performed on a (±)**2**·2H_2O sample.

process	rate K/min	modification 1			modification 2		
		temp.interval *T*/ K	T_{peak} K	ΔH^o J/g	temp.interval *T*/ K	T_{peak} K	ΔH^o J/g
1st cooling	5						
1st heating	10	196.8→ 226.1	201.6	2.6	257.7→ 286.1	267.3	1.6
2nd cooling	10						
2nd heating	10	196.5 → 224.2	201.6	2.7	251.8 →295.7	274.0	3.8
3rd cooling	20						
3rd heating	10	202.2 → 223.3	207.4	0.5	257.6 →292.9	270.6	2.7

Again, two enthalpic modifications are observed in three different heating processes at 10 K/min. Increasing cooling rates have been used before each heating process.

When submitted to DSC experiments, equivalent modifications are observed and shown in Table 2. It can be noted that the temperature intervals are shorter in the case of **modification 1**.

2.3 Loss of water content of (±)**1**·2H_2O and (±)**2**·2H_2O observed by DSC and TG

For compound (±)**1**·2H_2O, DSC experiments in the temperature interval 283 K - 363 K were made at a heating rate of 10 K/min. Before being submitted to the heating process, the sample was equilibrated inside the calorimeter at T = 283 K. Only one peak over the temperature range 326 K - 364 K (T_{peak}= 350.1 K), was observed, corresponding to a loss of mass of 13.6% for the sample. In order to study the reversibility of this process the sample was immediately submitted to a cooling and second heating runs under the same conditions and no thermal effect was found in any of the records, indicating that the thermal effect found in the first heating can be associated with the loss of two water molecules (theoretical mass loss, 13.0%).

A similar phenomenon was also observed by DT/TGA measurements, in which the mass loss between 333 K - 393 K results in a 13.7%, again consistent with the loss of two water molecules.

[7] Höhne, G.W.H.; Hemminger, W.F.; Flammersheim, H.-J.; "Differential Scanning Calorimetry", 2nd edition, Springer, Berlin **2003**, p. 229.

The DSC measurements of compound (±)**2**·2H_2O in the interval 283 K - 343 K show the dehydration endotherm over the temperature range 310 K - 338 K (T_{peak} = 329.4 K), corresponding to a 11.7% of mass loss. The theoretical calculated value for the loss of two water molecules is 11.9%, that is, in both compounds the relation water/monomer is 2/1.

2.4 Experimental

2.4.1 DSC Experiments

The behavior of the sample as a function of the temperature was studied by Differential Scanning Calorimetry. Two DSC apparatus were used for the measurements. For experiments at lower temperatures (from 150 K to 298 K) a Mettler DSC30 was used. For experiments made in the temperature interval 283 K to 363 K a Pyris1 instrument from Perkin Elmer was used. Both instruments were previously calibrated in temperature and energy with reference materials.[8] The standards used for calibration were hexafluorobenzene, 99.9 % purity, supplied by Aldrich; benzoic acid NIST standard reference sample 39j; and high-purity indium (mass fraction: > 0.99999) and tin supplied by Perkin-Elmer. In all the experiments the samples were examined in non hermetically sealed pans and in nitrogen atmosphere. Samples were weighed before and after the runs with a Mettler AT21 microbalance, sensitivity ±0.000002 g.

For the experiments at lower temperatures the sample was equilibrated inside the calorimeter at T = 298 K and then cooled at a rate of 5 K/min until 150 K. The cooled sample was afterwards subjected to a heating run at a rate of 10 K/min and two broad peaks corresponding to two different processes (modifications) were found. In order to study the reversibility of the observed behavior and the influence of the rate of cooling, the sample was subjected to cooling at a rate of 10 K/min followed by heating at 10 K/min, and newly cooled at a rate of 20 K/min followed by a heating rate of 10 K/min. As the results are reproduced, the processes are reversible.

For the experiments in the temperature interval from 283 K to 363 K samples were equilibrated inside the calorimeter at T = 283 K before being submitted to the heating process. In order to study the reversibility of this process, samples were immediately

[8] (a) Gmelin, E.; Sarge, S.M. *Thermochim. Acta,* **2000**, *347*, 9-13. (b) Sarge, S.M.; Gmelin, E.; Höhne, G.W.H.; Cammenga, H.K.; Hemminger, W.; Eysel, W.; *Thermochim. Acta.* **1994**, *247*, 129-168. (c) GEFTA (Gesellschaft für Thermische Analyse, Germany), Gmelin, E.; Sarge, S.M. *Pure Appl. Chem*. **1995,** *67,* 1789-1800. (d) Sabbah, R.; Xu-wu, A.; Chickos, J.S.; Planas Leitão, M.L.; Roux, M.V.; Torres, L.A.; *Thermochim. Acta,* **1999**, *331*, 93-204.

submitted to a cooling and a second heating runs under the same conditions and no thermal effect was found in any of the records, indicating that the thermal effect observed in the first heating was associated with the irreversible loss of water.

In the case of (±)**1**·2H_2O, the sample was kept in a box with a relative humidity of 92 % over 50 days in order to study the possible reversibility of the process by introduction of water in the molecule. The weight of the sample and a new DSC run showed that the loss of water is irreversible.

2.4.2 TG Experiments

Experiments were carried out in a DSC Seiko calorimeter, with a TG/DTA 6200 thermogravimetry accessory. Non hermetically sealed aluminium pans were used for introducing 1.99087 mg of (±)**1**·2H_2O. Results were obtained employing a heating rate of 5 K/min.

3 Analytical Data for Compound (±)**2**·2H_2O

3.1 Experimental procedure and spectroscopic and physical data

Compound **2** was synthesized by condensing the dilithium salt of 3-methylene-cyclohexanecarboxylic acid with hepta-1,6-dien-4-one following the synthetic sequence reported for other members of this family of compounds.[9] Single crystals of compound **2** suitable for X-ray analysis were grown at room temperature from a damp carbon tetrachloride/2,2,4-trimethylpentane mixture (4:1), after several days.

(1*R,5*R**)-7,7-Diallyl-5-hydroxymethyl-6-oxabicyclo[3.2.1]octane-1-carboxylic Acid (2).** Crystalline solid: mp 72.8-73.5 ˚C; R_f 0.60 (ethyl acetate); IR (KBr) 3732(w), 3390 (br), 3075 (m), 2959 (s), 2869 (m), 2641 (br), 2360 (s), 1670 (s), 1638 (m), 1434 (m), 1045 (s), 773 (s) cm^{-1}; ^1H NMR ($CDCl_3$, 500 MHz) δ 5.99 (ddd, *J* = 10.0, 7.0, 7.0 Hz, 1H), 5.89 (ddd, *J* = 10.0, 7.0, 7.0 Hz, 1H), 5.15-5.02 (m, 4H), 3.56 (d, *J* = 11.8 Hz, 1H), 3.42 (d, *J* = 11.8 Hz, 1H), 2.88 (ddd, *J* = 12.0, 2.5, 2.5 Hz, 1H), 2.71 (br d, *J* = 7.0 Hz, 2H), 2.40 (br d, *J* = 7.0 Hz, 2H), 2.30 (br ddd, *J* = 11.0, 10.7, 2.5 Hz, 1H), 2.10-1.95 (m, 1H), 1.81-1.73 (m, 1H), 1.75-1.67 (m, 1H), 1.57 (br dd, *J* = 12.4, 7.5 Hz, 1H), 1.45 (d, *J* = 12.0 Hz, 1H), 1.29 (ddd, *J* = 13.0, 11.7, 7.0 Hz, 1H); ^{13}C NMR ($CDCl_3$, 125 MHz) δ 178.5, 134.5, 134.4, 118.0, 117.9, 85.4, 83.2, 66.3, 55.9, 42.4, 39.8, 37.9, 32.0, 31.2, 19.1. Anal. Calcd for $C_{15}H_{24}O_5$: C, 63.36; H, 8.51. Found: C, 63.42; H, 8.34.

[9] Carrasco, H; Foces-Foces, C.; Pérez, C.; Rodríguez, M.L.; Martín, J.D. *J. Am. Chem. Soc.* **2001**, *123*, 11970-11981.

3.2 Crystal structure data for (±)**2**·2H_2O at 170 K

(Further details of the data collection and structure solution of (±)**2**·2H_2O at 293, 170 and 115 K are provided in CIF)

Crystal data and structure refinement parameters for (±)**2**·2H_2O at 170 K

Identification code	f23lt	
Empirical formula	C15 H26 O6	
Formula weight	302.36	
Temperature	170(2) K	
Wavelength	0.71073 Å	
Crystal system	Trigonal (hexagonal axis)	
Space group	R-3	
Unit cell dimensions	a = 35.405(5) Å	α= 90°.
	b = 35.405(5) Å	β= 90°.
	c = 6.6260(5) Å	γ = 120°.
Volume	7193.0(14) $Å^3$	
Z	18	
Density (calculated)	1.256 Mg/m^3	
Absorption coefficient	0.096 mm^{-1}	
F(000)	2952	
Theta range for data collection	1.99 to 27.50°.	
Reflections collected	3632	
Completeness to theta = 27.50°	99.0 %	
Refinement method	Full-matrix least-squares on F^2	
Final R indices [I>2sigma(I)]	R1 = 0.0909, wR2 = 0.2387	
R indices (all data)	R1 = 0.1128, wR2 = 0.2544	
Largest diff. peak and hole	1.479 and -0.285 $e.Å^{-3}$	

Table 3: (±)**2**·2H_2O at 170 K

O(6)-O(6)#1	2.697(9)
O(6)-O(6)#2	2.736(7)
O(6)-O(6)#3	2.736(7)
O(7)-O(8)#4	1.45(6)
O(7)-O(8)#1	1.45(6)
O(8)-O(6)#2	1.619(13)
O(8)-O(8)#4	2.90(11)
O(6)#1-O(6)-O(6)#2	90.0
O(6)#2-O(6)-O(6)#3	60.0
O(8)#4-O(7)-O(8)#1	0.0
O(8)#1-O(7)-O(8)	180.0

Selected bond lengths [Å] and angles [°] for the disorder water molecule inside the channel. Occupancy factors of 0.747(11), 0.178(12) and 0.079(9) for O6, O7 and O8 respectively. Symmetry transformations used to generate equivalent atoms: #1 y+1/3,-x+y+2/3,-z-1/3 #2 -y+1,x-y,z #3 -x+y+1,-x+1,z #4 -x+4/3,-y+2/3,-z-1/3

Table 4: (±)**2**·2H_2O at 170 K .Selected torsion angles [°] defining the conformation of the substituents

C(1)-C(2)-C(3)-C(4)	-39.0(4)
C(4)-C(5)-C(7)-O(3)	-50.1(4)
C(4)-C(5)-C(7)-O(4)	127.7(3)
O(1)-C(1)-C(8)-O(2)	55.4(4)

Table 5: Hydrogen bonds for (±)**2**·2H_2O at 170 K [Å and °].

D-H...A	d(D-H)	d(H...A)	d(D...A)	<(DHA)
O(2)-H(2)...O(3)#6	0.84	2.00	2.790(4)	157
O(4)-H(4)...O(5)#7	0.84	1.76	2.602(4)	176
O(5)-H(5WB)...O(1)	0.82(1)	1.94(1)	2.749(3)	169(5)
O(5)-H(5WA)...O(2)#8	0.82(1)	1.95(1)	2.772(3)	176(5)

Symmetry transformations used to generate equivalent atoms:

#1 y+1/3,-x+y+2/3,-z-1/3 #2 -y+1,x-y,z #3 -x+y+1,-x+1,z #4 -x+4/3,-y+2/3,-z-1/3

#5 x-y+1/3,x-1/3,-z-1/3 #6 x-y+1/3,x-1/3,-z+2/3 #7 y+1/3,-x+y+2/3,-z+2/3

#8 x,y,z-1

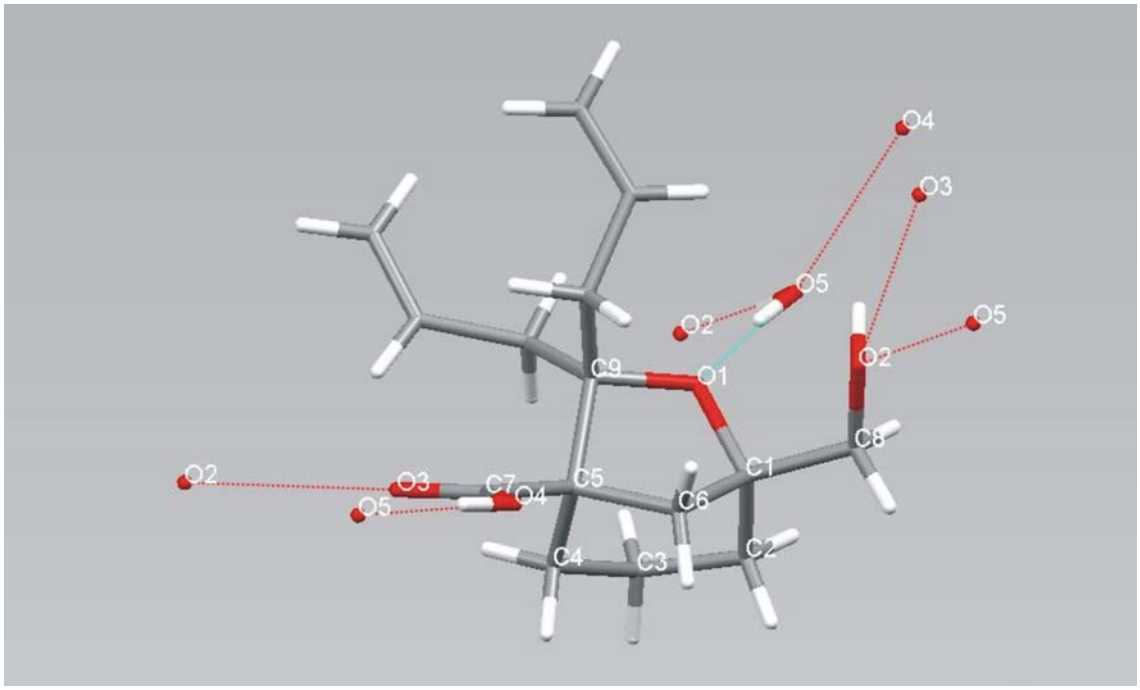

Figure 5: Molecular structure of compound (±)**2**·2H_2O at 170 K showing the numbering system and the O-H…O hydrogen interactions

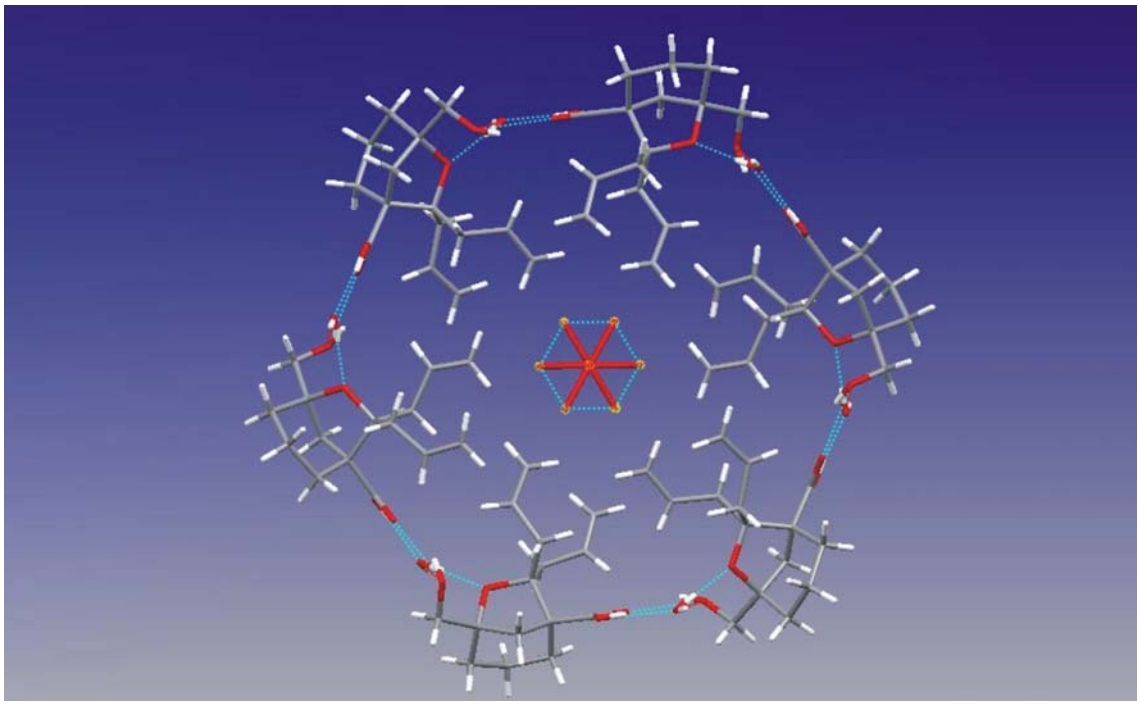

Figure 6: Macro-ring system ((±)**2**·2H_2O, 170 K) showing the hydrogen bonds and the disorder of the water molecule inside the channel.

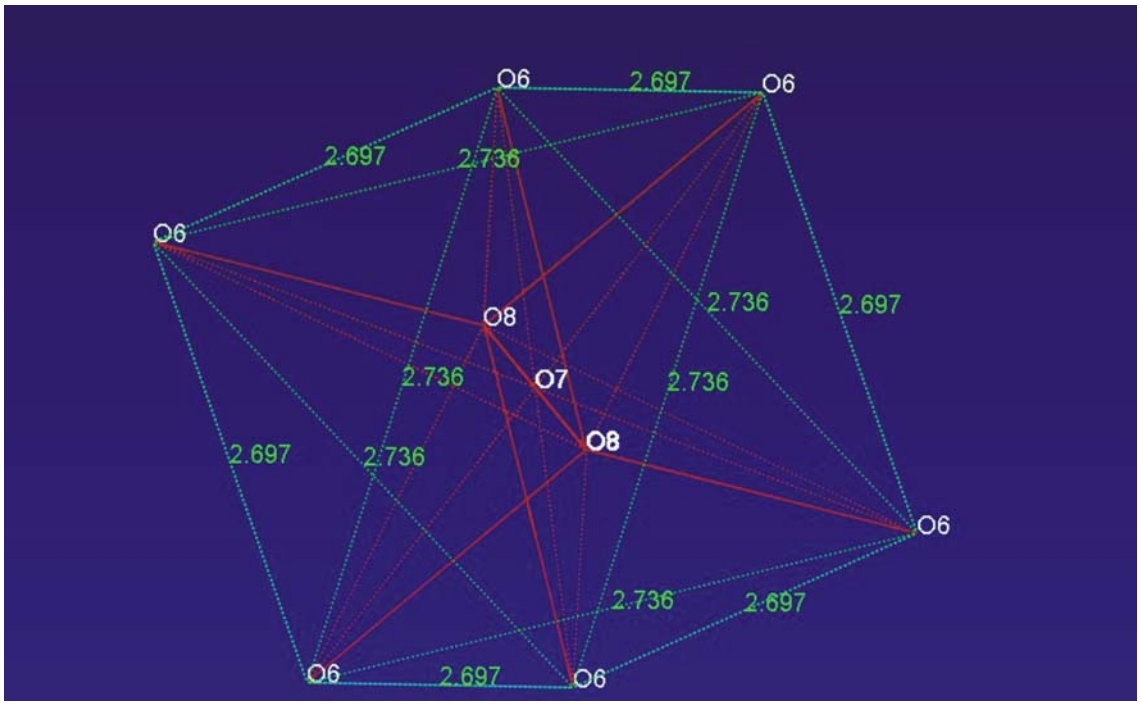

Figure 7: Disordered water molecule inside the channel ((±)**2**·2H_2O, 170 K) with occupancy factors of 0.747(11), 0.178(12) and 0.079(9) for O6, O7 and O8 respectively. The bond distances for the disordered water molecule O6 forming the octahedral are also shown.

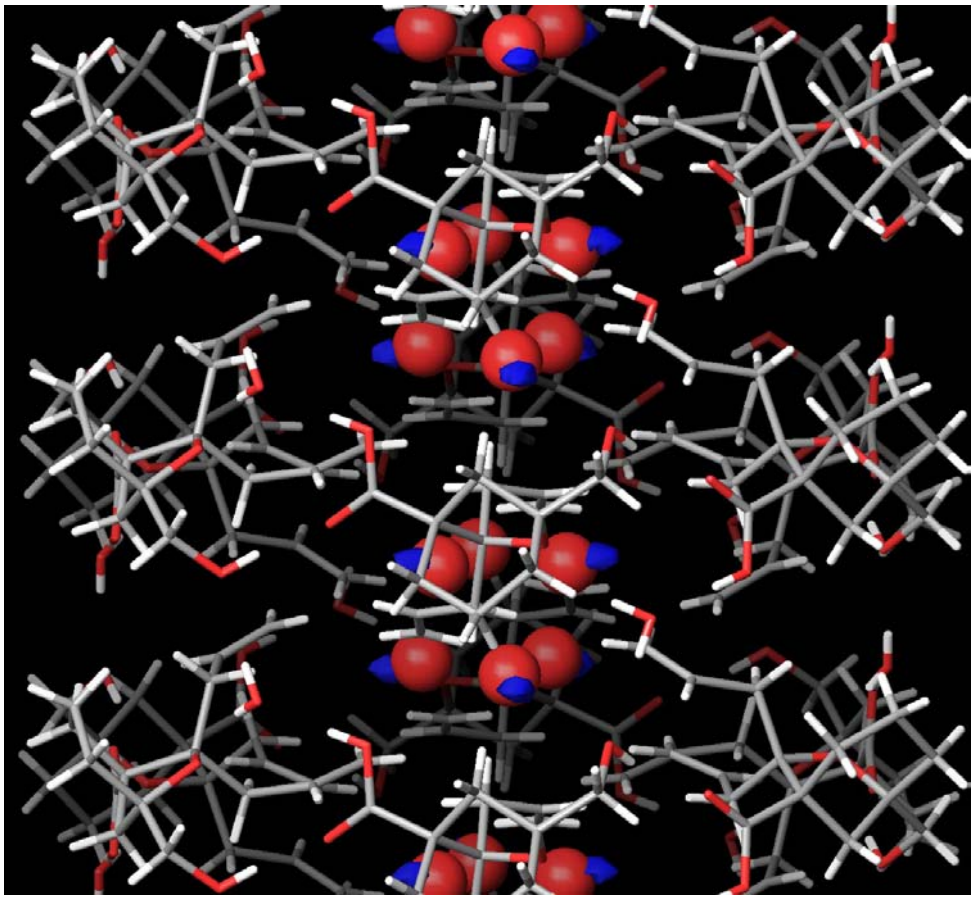

Figure 8: Location of discrete water clusters in the pore formed by (±)**2**·2H_2O (side view). Compound **2** and structural water in capped sticks, water molecules forming cage hexamers are shown as red spheres. Water-binding regions marked in blue (isosurface at -2.2 kcal/mol level), were calculated using SiteMap as implemented in MAESTRO 7.5[10] (dipole method, 20 Å atom cutoff, 0.25 Å grid spacing). The availability of these hydrophilic nodes should reduce the energy barrier to water permeability across this otherwise predominantly hydrophobic pathway.

[10] MAESTRO, versión 7.5, Schrödinger, LLC, New York, 2005.